

Temperature-dependent photoluminescence and electron field emission properties of AlN nanotip arrays

X. H. Ji,¹ Q. Y. Zhang,^{1,a)} S. P. Lau,^{2,b)} H. X. Jiang,³ and J. Y. Lin³

¹MOE Key Laboratory of Specially Functional Materials, South China University of Technology, Guangzhou 510641, People's Republic of China

²Department of Applied Physics, The Hong Kong Polytechnic University, Hung Hom, Kowloon, Hong Kong

³Department of Physics, Kansas State University, Manhattan, Kansas 66506-2601, USA

(Received 24 January 2009; accepted 5 April 2009; published online 28 April 2009)

Large-scale single-crystalline AlN nanotip arrays have been fabricated via a facile catalysis-free approach using AlCl₃ powder and NH₃ as starting materials. These nanotips exhibit an intense broad ultraviolet emission centered at 3.28 eV. The field emission features a notable electron current with a low turn-on field. The turn-on and threshold electric field are found to decrease substantially from 7.7 to 3.9 V/μm and 7.9 to 4.1 V/μm, respectively, while the estimated field enhancement factor increases from 483 to 1884 with increasing the ambient-temperature from room temperature to 573 K. The dependence of the photoluminescence and electron field emission with temperature and the possible mechanism involved has systematically been investigated and thus discussed. © 2009 American Institute of Physics. [DOI: 10.1063/1.3126055]

The recent demonstration of advanced nanodevice prototypes including field effect transistors, polarization-sensitive nanoscale photodetectors, and ultraviolet (UV) nanowire nanolasers has been considered as an exciting scenario toward the development of modern nanoscience and nanotechnology.^{1–3} It is indeed great and quite inspiring advancement of the modern nanotechnology, various one-dimensional (1D) nanomaterials have therefore been fabricated ranging from elementary substances² to complex compounds⁴ and even to superlattices.⁵ As an important member of the promising semiconductors group-III nitrides, aluminum nitride (AlN) is characterized by its direct band gap of 6.1 eV, small or even negative electron affinity as well as its attractive thermal conductivity, chemical stability, and mechanical strength.⁶ Nanostructured AlNs have long been viewed as promising materials for photonics and electronic applications, e.g., compact high-efficiency UV light-emitting diodes and laser diodes, flexible pulse-wave sensors, and nanomechanical resonators.⁷ To date a variety of 1D AlN nanostructures have been developed, for instance, nanowires, nanocones, nanobelts, nanoneedles, nanorods, and nanotips.^{8–15} Among others, electron emitters with high aspect ratio tips, predicted by the modified Fowler–Nordheim (FN) equation,^{16,17} can greatly facilitate field emission (FE) at low turn-on voltages. Thus AlN nanotips have been regarded as favorable candidates for scanning probes and field emitters. Moreover their excellent radial rigidity largely eliminates the noise and poor signals caused by the otherwise unwanted mechanical or thermal vibration.^{9,10}

Herein, the main objective of this letter is to carry out a study on structural and temperature-dependent photoluminescence (PL) and FE properties of aligned large-scale single-crystalline AlN nanotip arrays, to examine their suitability as potential light and electron emission nanodevices. The temperature dependence of the PL and FE properties and also the possible mechanisms involved have been investi-

gated and discussed. Acquisition knowledge of aligned large-scale 1D AlN nanotip arrays and their temperature-dependent physical properties are of important steps in realizing their applications in electronic/photonics nanodevices.

The AlN nanotips were prepared through a combined vapor transport and condensation process.^{17,18} Aluminum chloride (AlCl₃) powder and ammonium (NH₃) were used as starting materials. A clean Si(100) substrate was placed in a quartz tube at 4–5 cm away from the source materials. The AlCl₃ was loaded into a ceramic boat and placed into the center of the quartz tube. After the furnace was pumped down to ~10⁻³ Torr, NH₃ at 50 (SCCM) (SCCM denotes standard cubic centimeters per minute at STP) was introduced into the tube. When the temperature of the furnace reached 1000 °C, the quartz tube was pushed into the hot zone of the furnace where the source material was located at the center of the furnace. The growth was maintained for 2 h at 1000 °C.

Shown in the inset of Fig. 1(a) is the typical x-ray diffraction (XRD) pattern of the obtained AlN nanostructures. The XRD pattern agrees well with the standard wurtzite AlN,¹⁹ revealing a wurtzite AlN structure with the lattice parameters of $a=0.3114$ nm and $c=0.4979$ nm. The strong intensity of the (002) peak indicates that the AlN nanocrystals grew preferentially along the c -axis. Figures 1(a) and 1(b) show the plain- and tilted-view scanning electron microscopy (SEM) images of AlN nanotips, from which one can see that the morphology of the nanotips are uniform with diameter around 10 nm at the tip and length more than a few hundred nanometers. The aspect ratio of each AlN nanotip is about 200, which is adequate for a FE application. To determine the detailed crystalline structure, transmission electron microscopy (TEM) was employed to investigate the nanotips. Hexagonal cross sections and layer-stacked structure along the growth direction are clearly observed from the typical low-magnification TEM images of the AlN nanotips, as shown in Figs. 1(c) and 1(d). The high-resolution TEM (HRTEM) of the 1D AlN nanotips are shown in the Figs. 1(e)–1(i). The hexagonal cross sections and layer-stacked

^{a)}Electronic mail: qyzhang@scut.edu.cn.

^{b)}Electronic mail: apsplau@polyu.edu.hk.

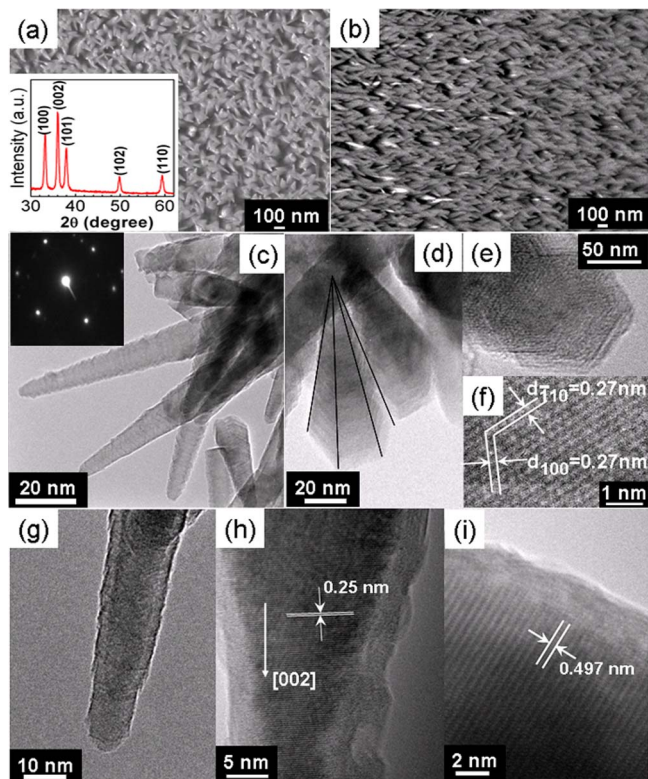


FIG. 1. (Color online) [(a) and (b)] The typical plain- and tilted-view low-magnification SEM images of the large-scale AlN nanotips, inset in Fig. 1(a) shows XRD pattern of AlN nanotips. [(c) and (d)] Typical low-magnification TEM image of the AlN nanotips, inset in (c) shows a SAED pattern of the single-crystalline AlN nanotips. [(e)–(i)] High-resolution lattice images of the AlN nanotips. [(e) and (f)] An enlarged view of the bottom of a typical AlN nanotip. [(g)–(i)] An enlarged view of the top-tip of a typical AlN nanotip, reveal that the nanotip is single-crystalline and has grown in the [001] direction, the lattice spacing in (002) is 0.25 nm.

structure have also been observed from the HRTEM image, as shown in Fig. 1(e). The distance between the neighboring lattice fringes of the hexagon cross section is about 0.27 nm, as shown in Fig. 1(f). Figure 1(g) presents a typical TEM image of a single AlN nanotip. The lattice spacing has been found to be 0.25 nm [Fig. 1(h)], corresponding to that of (002) plains of wurtzite AlN. Combining TEM with the defocus of the selected area electron diffraction (SAED) technique, the nanotip is single-crystalline and has been grown in the [002] direction.

Deep UV PL spectroscopy under a 197 nm laser excitation was employed to study the optical properties of the nanotips from 10 to 300 K. Figure 2(a) presents the temperature-dependent PL spectra of the AlN nanotips in the range of 2.5–6.2 eV measured at 10 and 300 K, respectively. The AlN nanotips exhibit an intense PL band centered at 3.28 eV, along with a weak shoulder located at 4.32 eV and an even weaker near band-edge emission at 5.83 eV at 300 K. The intense emission in the UV range indicates that these nanotips have potential applications in development of UV-light emitting devices. It can be observed that the UV emission becomes much stronger and exhibits a small blueshift with a decrease in the temperature from 300 to 10 K. Oxygen is one of the critical native defects for AlN, forming the O_N defects substituting for the nitrogen. O_N in the AlN lattice leads to the formation of V_{Al} due to the charge compensation.²⁰ O_N ions together with the Al vacancy (V_{Al})

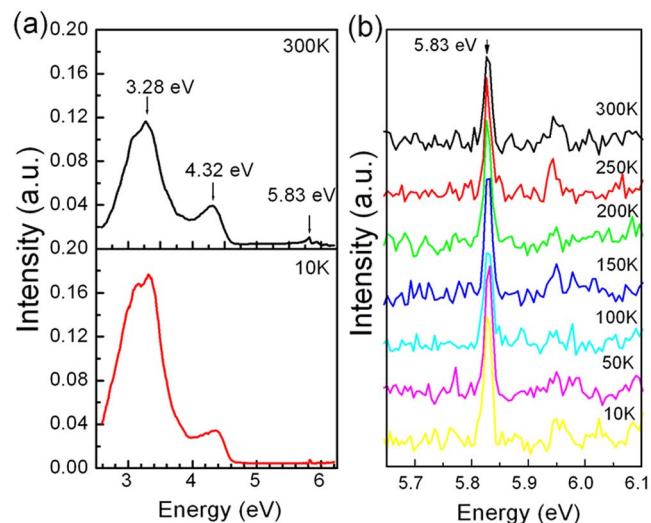


FIG. 2. (Color online) (a) Temperature-dependent PL spectra of the AlN nanotips in the range of 2.5–6.2 eV measured at 10 and 300 K. (b) An enlarged view of the temperature-dependent PL and the $\ln(I)-1/T$ plot of the 5.83 eV emission.

could be forming with oxygen-related point defects, which are responsible for the observation of luminescence at 3.28 and 4.32 eV.²¹ An enlarged view of the temperature-dependent PL of the 5.83 eV emission has been shown in Fig. 2(b). It is found that the peak position of the 5.83 eV emission exhibits no shift with the decrease in the temperature. Due to the absence of redshift of the defect emission with increasing temperature, it is likely that the observed emissions are not due to the direct transition between the electron in the conduction band and the deep level.

To assess the performance of the 1D AlN nanotips as a field emitter, FE properties were measured with a high vacuum level around 10^{-7} torr at different controlled temperatures. The measurement was conducted on a standard parallel-plate-electrode configuration where the indium-tin-oxide glass substrate was used as the anode as shown in the inset of Fig. 3(a). The anode was separated from the nanotips surface by a 120 μm gap using a Teflon film as spacer. Both the anode and the cathode were connected to a computer-controlled Keithley 248 source meter. The diameter of the current emission area was 5 mm. Figure 3(a) shows the dependence of FE current density J on the applied electric field strength E of the 1D AlN nanotip arrays for different temperatures. The turn-on electric field ($E_{\text{turn-on}}$) and threshold electric field (E_{th}) of the AlN nanotips based on the 10 $\mu\text{A}/\text{cm}$ and 1 mA/cm^2 current density criterion are 7.7 and 7.9 $\text{V}/\mu\text{m}$ at RT, respectively. The exponential dependence between the emission current and the applied field for different temperatures, plotted in $\ln(J/E^2)-1/E$ relationship are presented in Fig. 3(b). It is noted that the emission current density J is exponentially raised with the increase in applied field E . It is interesting to note that the turn-on and threshold electric fields decrease substantially from 7.7 to 3.9 $\text{V}/\mu\text{m}$ and 7.9 to 4.1 $\text{V}/\mu\text{m}$ with an increase in temperature from RT to 573 K. Meanwhile the emission current density increases significantly with the temperature change, as shown in Fig. 3(a). For example, to get emission current density $J=1$ A/cm^2 , 8.4 $\text{V}/\mu\text{m}$ field is needed for the AlN nanotips at RT but only 4.8 $\text{V}/\mu\text{m}$ field is needed for the same current density at 573 K. The work function of mate-

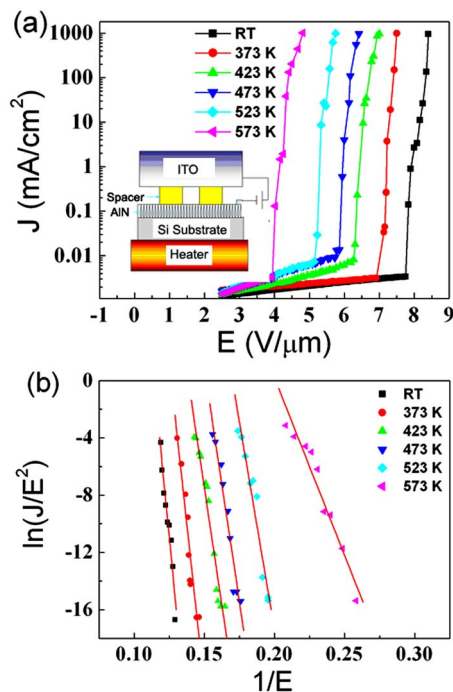


FIG. 3. (Color online) The dependence of the FE current density J on the applied electric field strength E of the AIN nanotips for different temperatures. (a) J - E plot, inset shows configuration of the AIN nanotips for FE and (b) FN relationship of $\ln(J/E^2) - 1/E$ plot.

rials is strongly temperature dependent. Thus the decrease of turn-on field and the increase in emission current density with the increase in the temperature might be due to the decrease in the effective work function of the AIN nanotips.

To test whether the electron emission is originated from electron tunneling, the FN equation is commonly used to examine the tunneling phenomena.²² Whenever the $\ln(J/E^2)$ versus $1/E$ plot yields a straight line, then the electrons are considered to be emitted through tunneling of the energy barrier. For temperature-dependent FE, total current density, J (in A/cm^2), is given by a simplified FN equation and Richardson–Dushman equation as²³

$$J = J_E + J_T, \quad (1)$$

where J_E and J_T are the field current and thermoionic current density, respectively. For AIN with a work function of 3.7 eV and temperature below 1000 K, the highest contribution of thermionic emission is much smaller than the FE current density, that is, the measured emission property is predominated by FE current because below 1000 K, the thermoionic emission effect is less significant than the FE effect.^{23,24}

From the slope of the $\ln(J/E^2) - 1/E$ plot, the estimated field enhancement factor β is found to lie in the range of 483–1884 with an increase in the temperature from RT to 573 K. The effective work function, ϕ_e , is relative with the true work function through the relation $\phi_e = \phi/\beta^{2/3}$,²⁴ and is found to lie in the range of 0.060–0.024 eV for the AIN nanotips with different ambient temperatures. The field enhancement factor increases while the effective work function decreases monotonously with the temperature, which ex-

plains very well the increase in emission current density with measuring temperature. The variation of the emission current density of the AIN nanotip arrays has also been measured at RT. No obvious degradation of current density has been observed and the emission current fluctuation has been found to be less than 8% at $8.0 V/\mu m$ in 1000 min. The observed stable FE behavior could be suggested to be related to the large-scale and uniform AIN nanotip arrays, which guarantees a uniform field distribution across the device under test.

In summary, we conclude that a facile catalysis-free vapor phase approach has been developed to produce large-scale and uniform 1D single crystalline AIN nanotips using $AlCl_3$ and NH_3 as starting materials. Nanostructural characterization shows that the nanotips are in the diameter of 10 nm with [001] growth direction and length extending a few hundred nanometers. The PL and FE characterizations reveal that these AIN nanotip arrays have exhibited broad UV-blue emissions and with a good FE property, thus suggesting a strong potential for their applications in light and FE nanodevices.

¹C. Liu, Z. Hu, Q. Wu, X. Z. Wang, H. Sang, J. M. Zhu, S. Z. Deng, and N. S. Xu, *J. Am. Chem. Soc.* **127**, 1318 (2005).

²A. M. Morales and C. M. Lieber, *Science* **279**, 208 (1998).

³M. H. Huang, S. Mao, H. Feick, H. Q. Yan, Y. Y. Wu, H. Kind, E. Weber, R. Russo, and P. D. Yang, *Science* **292**, 1897 (2001).

⁴X. F. Duan, Y. Huang, Y. Cui, J. F. Wang, and C. M. Lieber, *Nature (London)* **409**, 66 (2001).

⁵J. T. Hu, M. Ouyang, P. D. Yang, and C. M. Lieber, *Nature (London)* **399**, 48 (1999).

⁶M. E. Levinstein, S. L. Ramyantsev, and M. S. Shur, *Properties of Advanced Semiconductor Materials* (Wiley, New York, 2001).

⁷Y. Taniyasu, M. Kasu, and T. Makimoto, *Nature (London)* **441**, 325 (2006).

⁸M. Kuball, J. M. Hayes, A. D. Prins, N. W. A. van Uden, D. J. Dunstan, Y. Shi, and J. H. Edger, *Appl. Phys. Lett.* **78**, 724 (2001).

⁹Y. B. Tang, H. T. Cong, Z. G. Chen, and H. M. Cheng, *Appl. Phys. Lett.* **86**, 233104 (2005).

¹⁰Q. Zhao, J. Xu, X. Y. Xu, Z. Wang, and D. P. Yu, *Appl. Phys. Lett.* **85**, 5331 (2004).

¹¹J. H. He, R. Yang, Y. L. Chueh, L. J. Chou, L. J. Chen, and Z. L. Wang, *Adv. Mater. (Weinheim, Ger.)* **18**, 650 (2006).

¹²V. N. Tondare, C. Balasubramanian, S. V. Shende, D. S. Joag, V. P. Godble, and S. V. Bhoraskar, *Appl. Phys. Lett.* **80**, 4813 (2002).

¹³S.-C. Shi, C.-F. Chen, S. Chattopadhyay, K.-H. Chen, and L. C. Chen, *Appl. Phys. Lett.* **87**, 073109 (2005).

¹⁴J. Zheng, Y. Yang, B. Yu, X. Song, and X. Li, *ACS Nano* **2**, 134 (2008).

¹⁵N. Muradov and A. Schwitter, *Nano Lett.* **2**, 673 (2002).

¹⁶L. Vila, P. Vincent, L. D. Pra, G. Pirio, E. Minoux, L. Gangloff, S. Demoustier-Champagne, N. Sarazin, E. Ferain, R. Legras, L. Piraux, and P. Legagneux, *Nano Lett.* **4**, 521 (2004).

¹⁷C. X. Xu and X. W. Sun, *Appl. Phys. Lett.* **83**, 3806 (2003).

¹⁸X. H. Ji, S. P. Lau, S. F. Yu, H. Y. Yang, T. S. Heng, and J. S. Chen, *Nanotechnology* **18**, 105601 (2007).

¹⁹JCPDS Card No. 25–1133.

²⁰M. S. Liu, L. A. Brusill, S. Praver, K. W. Nugent, Y. Z. Tong, and G. Y. Zhang, *Appl. Phys. Lett.* **74**, 3125 (1999).

²¹R. A. Youngman and J. H. Harris, *J. Am. Ceram. Soc.* **73**, 3238 (1990).

²²F. Liu, J. F. Tian, L. H. Bao, T. Z. Yang, C. M. Shen, X. Y. Lai, Z. M. Xiao, W. G. Xie, S. Z. Deng, J. Chen, J. C. She, N. S. Xu, and H. J. Gao, *Adv. Mater. (Weinheim, Ger.)* **20**, 2609 (2008).

²³S. F. Ahmed, S. Das, M. K. Mitra, and K. K. Chattopadhyay, *Appl. Surf. Sci.* **254**, 610 (2007).

²⁴M. C. Kan, J. L. Huang, J. C. Sung, K. H. Chen, and B. S. Yau, *Carbon* **41**, 2839 (2003).